Anomalous Joule law in the adiabatic dynamics of a quantum dot in contact with normal-metal and superconducting reservoirs

Liliana Arrachea[1,2] and Rosa López[3]

[1]*International Center for Advanced Studies, Escuela de Ciencia y Tecnología, Universidad Nacional de San Martín, 25 Avenida de Mayo y Francia, 1650 Buenos Aires, Argentina*

[2]*Dahlem Center for Complex Quantum Systems and Fachbereich Physik, Freie Universität Berlin, 14195 Berlin, Germany*

[3]*Institut de Física Interdisciplinària i de Sistemes Complexos (CSIC-UIB), 07122 Palma de Mallorca, Spain*

(Received 9 April 2018; published 5 July 2018)

We formulate a general theory to study the time-dependent charge and energy transport of an adiabatically driven quantum dot in contact with normal and superconducting reservoirs at $T = 0$. This setup is a generalization of a quantum RC circuit, with capacitive components due to Andreev processes and induced pairing fluctuations, in addition to the conventional normal charge fluctuations. The dynamics for the dissipation of energy is ruled by a Joule law for four channels in parallel with the universal Büttiker resistance $R_0 = e^2/2h$ per channel. Two transport channels are associated with the two spin components of the usual charge fluctuations, while the other two are associated with electrons and holes due to pairing fluctuations. The latter leads to an "anomalous" component of the Joule law and takes place with a vanishing net current due to the opposite flows of electrons and holes.

DOI: 10.1103/PhysRevB.98.045404

I. INTRODUCTION

Time-dependent transport at the nanoscale is a prominent tool for probing electronic dynamics at very low temperatures. A prototypical instance is found in on-demand single-electron sources in which individual electron and hole charges are perfectly emitted [1]. The simplest device that works as a quantized emitter is a quantum capacitor, which consists of a single-level quantum dot tunnel coupled to a unique reservoir. In such a case only a purely ac current response is possible when the dot gate is electrostatically influenced by an ac voltage source [2–7]. Working in a range of gigahertz frequencies Ω and at sufficiently slow ac amplitudes V_g, this setup behaves as an RC circuit that for the quantum regime exhibits the peculiarity that relaxation processes are featured by a universal quantized resistance $R_0 = h/2e^2$ [2–4]. The quantum analog to the classical RC circuit is now done by replacing the geometrical capacitance by a quantum capacitance which is proportional to the density of states of the localized level.

Conductance quantization is observed in the stationary regime as a signature of ballistic transport due to the lack of backscattering events [8,9]. In a quantum capacitor operating in conditions where many-body interactions do not play a role, the resistance quantization is attributed to a particular behavior of the dwell time. R_0 is universal because the mean value for the square of the dwell time coincides with the square of its mean value. For interacting systems under ac driving charge relaxation processes are dictated by the correlation function of the electron-hole excitations, which are proportional to the available density of electron-hole pairs or, equivalently, to the charge susceptibility [10–20]. In that case, there is a relaxation resistance R_0 per spin channel and such universality resides in the fulfillment of the Korringa-Shiba relation [15,19–21]. The latter holds for systems that behave as Fermi liquids, which to some extent behave as noninteracting systems with renormalized parameters. In addition, a different quantization phenomenon in a quantum capacitor is observed, depending on the way in which the ac amplitude is increased beyond linear response [5–7,22–28]. Such quantization has potential metrological applications and is suitable for quantum computing designs. Most of the studies on quantum RC circuits

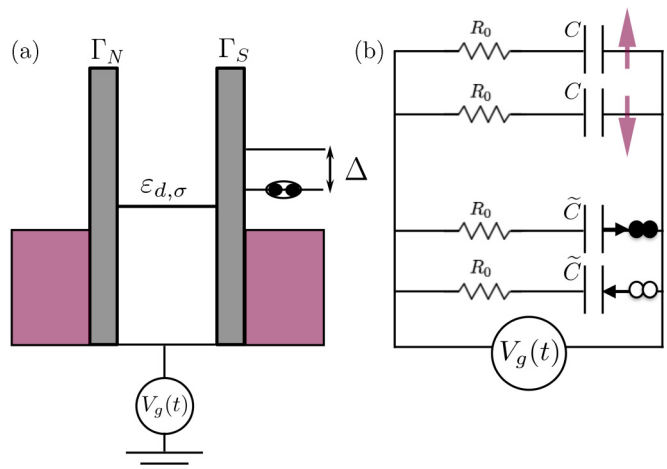

FIG. 1. (a) Sketch of the setup. A quantum dot is driven by an ac gate voltage $V_g(t) = V_0 \sin(\Omega t)$ and is connected to a normal lead and a superconducting lead. (b) Representation of the dynamics of the charge and energy by means of an effective circuit with capacitive and resistive elements. The two branches associated with the normal charge fluctuations are associated with the two components of the spin of the electrons. The other two describe the anomalous charge flow due to fluctuations of the induced pairing at the quantum dot. The corresponding charge fluxes are associated with electrons and holes and have opposite directions, as indicated by the solid-dot pairs (electrons) and open ones (holes).

belong to the linear regime, with the nonlinear regime being investigated less. In particular, few studies have been reported in the interacting system beyond linear response [28–31].

In the nonlinear regime, how to extend the concept of relaxation resistance is not obvious because the analogy to the classical circuit is not necessarily valid. Resistive behavior is related to dissipation of energy. Hence, the analysis of the energy transport and heat production in parallel with the charge transport in these systems is a natural strategy. In a recent work, it was shown that a noninteracting quantum dot driven in the adiabatic regime obeys an *instantaneous Joule law* with a universal resistance R_0 per transport channel [32–35]. For an interacting quantum dot described by the Anderson impurity model, the fact that the instantaneous susceptibility satisfies the Korringa-Shiba law ensures the validity of the same universal instantaneous Joule law. When a magnetic field is included in this model for the interacting quantum dot, the Joule law is not satisfied separately for each spin channel, but it is satisfied by the effective resistance of the two spin channels considered in a parallel circuit configuration [31].

A very interesting generalization of the RC circuit is to consider a configuration where the capacitive element, the quantum dot, is connected not only to a conducting lead but also to a superconducting one. The dc transport in setups containing a quantum dot embedded in a normal-superconductor (N-S) junction has been widely investigated theoretically and also experimentally [36–40]. Pumping induced by ac driving in quantum dots in N-S junctions has also been investigated [41–43]. However, RC configurations and time-dependent transport induced by a single driving potential in the quantum dot in these structures have been studied only recently [44]. The extra ingredient that the N-S coupling brings about is the conversion of electron-hole pairs into Cooper pairs between the two leads because of the Andreev processes [45], along with induced superconductivity at the quantum dot. The aim of the present work is to explore the impact that these effects have on the interplay between the charge and the energy dynamics of such hybrid RC setups. A sketch of the setup is shown in Fig. 1. We will focus on the adiabatic regime, where the period of the driving gate voltage is much larger than any characteristic time for the electrons in the quantum dot and both leads are at temperature $T = 0$. We will show that Andreev processes introduce an additional contribution to the quantum capacitance $C_{\mathrm{And}}(t)$, induced by the coupling to the normal lead $C_{\mathrm{N}}(t)$, while the induced pairing due to the coupling to the superconducting lead can be represented by an anomalous capacitance $\tilde{C}(t)$. The latter describes the simultaneous fluctuations of electrons and holes associated with the fluctuation of the induced pairing as a response to a variation of the gate voltage. Each of these capacitances depends on time in the regime where the amplitude of the driving voltage exceeds the range of linear response. The concomitant energy conversion can be described by an instantaneous Joule law. The latter is a generalization of the Joule law of Refs. [32–34], where, in addition to the contribution of the two spin channels, there is an anomalous component due to the disruption and formation of the induced pairing at the quantum dot. Unlike the former contribution, the latter takes place without a net charge flow since electrons and holes generate currents in opposite directions. The corresponding processes can be represented by the circuit in Fig. 1. This paper is organized as follows. In Sec. II we present the model. Section III contains the equations ruling the charge and energy dynamics, including the introduction of the adiabatic regime and the Green's function treatment to calculate the relevant time-dependent observables. The instantaneous Joule law is derived from the quantum dot dynamics in Sec. IV, while in Sec. V we show that the associated heat flows entirely into the normal lead. In Sec. VI we present some results that illustrate the behavior of the different components of the capacitances and the different components of the Joule heating. Finally, a summary and conclusions are presented in Sec. VII.

II. MODEL

We consider a single-level quantum dot that is tunnel coupled to both superconducting (S) and normal (N) reservoirs. The quantum dot is under the action of an oscillatory time-dependent gate potential $V_g(t) = V_0 \sin(\Omega t)$. The full setup is described by the Hamiltonian

$$H(t) = H_{\mathrm{d}}(t) + H_{\mathrm{N}} + H_{\mathrm{S}} + \sum_{\alpha=\mathrm{N,S}} H_{\mathrm{c}\alpha}. \tag{1}$$

The first term describes a single-level quantum dot,

$$H_{\mathrm{d}}(t) = \sum_{\sigma} [\varepsilon_{d,\sigma} + eV_g(t)] n_{d\sigma}, \tag{2}$$

where $d_\sigma^\dagger$ is the creation operator for an electron on the dot with spin $\sigma = \uparrow, \downarrow$ and $n_{d\sigma}$ denotes the occupation operator for spin σ. $\varepsilon_{d,\sigma}$ is the energy of the dot level, which is modulated by $V_g(t)$. The normal reservoir is described by a free-electron Hamiltonian,

$$H_{\mathrm{N}} = \sum_{\sigma,k\mathrm{N}} (\epsilon_{k\mathrm{N}} - \mu_N) c_{k\mathrm{N},\sigma}^\dagger c_{k\mathrm{N},\sigma}, \tag{3}$$

where $\epsilon_{k\mathrm{N}}$ is the energy dispersion relation, k is the wave vector, and $c_{k\mathrm{N},\sigma}$ is the destruction operator for an electron in the normal reservoir with spin σ. The electrochemical potential for the normal contact is represented by μ_N. The superconducting reservoir is described by a BCS Hamiltonian of the form

$$H_{\mathrm{S}} = \sum_{\sigma,k\mathrm{S}} [(\epsilon_{k\mathrm{S}} - \mu_S) c_{k\mathrm{S},\sigma}^\dagger c_{k\mathrm{S},\sigma} + \Delta c_{k\mathrm{S}\uparrow} c_{-k\mathrm{S},\downarrow} + \mathrm{H.c.}], \tag{4}$$

where Δ denotes the s-wave pairing potential for electrons at two states related by time reversal, denoted by $k\mathrm{S}\uparrow, -k\mathrm{S}, \downarrow$. The coupling between the dot and reservoirs is

$$H_{\mathrm{c}\alpha} = w_\alpha \sum_{k\alpha,\sigma} [c_{k\alpha,\sigma}^\dagger d_\sigma + \mathrm{H.c,}]. \tag{5}$$

Here, w_α is the tunneling amplitude that connects both the normal reservoir with the dot and the superconducting contact with the central site. We focus on the transport induced purely by the ac driving applied at the quantum dot, without any additional voltage bias applied at the leads. For simplicity, we consider $\mu_S = \mu_N = 0$.

III. CHARGE DYNAMICS AND DISSIPATION

In this section we formulate the equations describing the charge and energy dynamics of the full system. In the

forthcoming sections we will analyze the problem from two complementary perspectives: (i) First, we calculate the dot charge dynamics and the dissipated power in the adiabatic regime, and we show that both quantities are related by means of an instantaneous Joule law with a constant and universal resistance. Such a relation follows from a circuit description in which quasiparticles and pair generation events run in parallel (see Fig. 1). (ii) Second, we will focus on the case where the chemical potential lies within the gap of the S reservoir. Under these conditions, we calculate the heat flow at the normal contact and the charge current flow at the same lead. Again, we show a relationship between these two quantities given by an instantaneous Joule law. Remarkably, we arrive at this conclusion by evaluating the heat flow at the normal contact considering the contribution from the tunneling barrier, the energy reactance [32,35].

A. Charge and energy dynamics of the quantum dot

The quantum dot charge dynamics determines not only the charge current but also the amount of dissipated energy in the hybrid setup. Such dynamics is governed by a conservation law for the electrical charges. In this respect, the flow of charges across the quantum dot fulfills

$$e\dot{n}_d(t) = e\sum_\sigma \dot{n}_{d\sigma}(t) = -[I_{\rm N}(t) + I_{\rm S}(t)], \tag{6}$$

where $\dot{n}_{d\sigma}(t) \equiv -i/\hbar\langle[n_{d\sigma}, H]\rangle$ is the change in the occupation of the dot at time t corresponding to the spin σ and $e > 0$ is the electron charge. The charge currents flowing into the N and S leads are computed from the Heisenberg relation; they are

$$I_\alpha(t) = -ie/\hbar\langle[N_\alpha, H]\rangle, \tag{7}$$

with $\alpha = {\rm N,S}$ and $N_\alpha = \sum_{k\alpha,\sigma} c^\dagger_{k\alpha\sigma} c_{k\alpha\sigma}$ being the occupation operator for the normal and superconducting contacts.

The power supplied by the ac source is converted in electrical work done by the electrons at the rate

$$P(t) = -\left\langle \frac{\partial H}{\partial t}\right\rangle = -e\sum_\sigma n_{d\sigma}(t)\dot{V}_g(t). \tag{8}$$

This power equals the total heat production rate at time t [33],

$$\dot{Q}_{\rm tot}(t) = -P(t). \tag{9}$$

B. Spatial distribution of the heat flow

As explained in Refs. [16,33,34], the heat flow is instantaneously distributed in the different parts of the device, i.e., at the contacts, central site, and tunnel junctions, as follows:

$$\dot{Q}_{\rm tot}(t) = \sum_\alpha \left[J^E_\alpha(t) + J^E_{c\alpha}(t)\right] + \dot{E}_d(t), \tag{10}$$

where

$$J^E_\alpha(t) = -\frac{i}{\hbar}\langle[H_\alpha, H]\rangle, \quad J^E_{c\alpha}(t) = -\frac{i}{\hbar}\langle[H_{c\alpha}, H]\rangle \tag{11}$$

are the energy rate change at the reservoirs $\alpha \in N, S$ and the corresponding contacts. The change in the energy at the central site is

$$\dot{E}_d(t) = -\frac{i}{\hbar}\langle[H_d, H]\rangle + \left\langle\frac{\partial H}{\partial t}\right\rangle. \tag{12}$$

In Ref. [32], it was shown that, for a quantum dot connected to a normal lead, the most meaningful definition of the heat flux into the lead α is the one including the so-called energy reactance, $J^E_{c\alpha}(t)/2$, which is half of the energy rate change at the tunneling barriers. The latter represents the energy that is temporarily stored or emitted at the tunneling barrier. We adopt that definition and write the heat flux into the lead α as follows:

$$\dot{Q}_\alpha(t) = J^E_\alpha(t) + \frac{J^E_{c\alpha}(t)}{2}. \tag{13}$$

In the case of a dot connected to a single normal lead, the reactance ensures the validity of the second law of thermodynamics in the adiabatic regime [32–34]; it gives a proper description of the ac heat current spectrum in the linear response regime [16] and also of the transient dynamics [46]. Similarly, we can define the heat flow into the quantum dot [33,34] as

$$\dot{Q}_d(t) = \dot{E}_d(t) + \sum_\alpha \frac{J^E_{c\alpha}(t)}{2}. \tag{14}$$

Notice that, by substituting these definitions in Eq. (10) and using $\sum_\alpha ([H_\alpha, H] + [H_{c\alpha}, H]) + [H_d, H] = 0$, we get

$$\dot{Q}_{\rm tot}(t) = \sum_\alpha \dot{Q}_\alpha(t) + \dot{Q}_d(t) = -P(t), \tag{15}$$

which is, precisely, Eq. (9).

C. Adiabatic dynamics

We now focus on the so-called *adiabatic regime*, where the ac time is much longer than any other associated timescale for the setup. In this respect, the electron tunneling processes occur many times in an ac time period. For the description of the quantum dot dynamics in this regime we follow Refs. [31,47], where the quantum dot occupation is split into two contributions up to linear order in $\dot{V}_g(t)$. The adiabatic evolution of the occupancy of the quantum dot is given by

$$n_{d\sigma}(t) = n^f_{d\sigma}(t) + e\Lambda_\sigma(t)\dot{V}_g(t), \tag{16}$$

where $n^f_{d,\sigma}(t) \equiv \langle n_{d\sigma}\rangle_t$ is the snapshot occupancy of the dot, evaluated with the exact *equilibrium* density matrix ρ_t corresponding to the Hamiltonian $H(t)$ frozen at time t. The correction is linear both in the time variation of the ac amplitude and, equivalently, in the ac frequency Ω.

As a result of this expansion for the dot occupation one can show that the power developed by the ac source has a purely ac (Born-Oppenheimer) component $P_{\rm cons}(t)$ associated with the reversible heat produced by the conservative forces and a dissipative component $P_{\rm diss}(t)$ with a nonzero time average. The last term in Eq. (16) is associated with the frictional (dissipative) component of the force. In fact, by substituting Eq. (16) into Eq. (8) we find

$$P(t) = P_{\rm cons}(t) + P_{\rm diss}(t), \tag{17}$$

with

$$P_{\rm cons}(t) = e\sum_\sigma n^f_{d\sigma}(t)\dot V_g(t),$$
$$P_{\rm diss}(t) = e^2\sum_\sigma \Lambda_\sigma(t)[\dot V_g(t)]^2. \quad (18)$$

When performing the averages over one period $\tau = 2\pi/\Omega$,

$$\overline{P}_{\rm cons,diss} = (1/\tau)\int_0^\tau dt\, P_{\rm cons,diss}(t), \quad (19)$$

for these two contributions to the power, we can verify that $\overline{P}_{\rm cons} = 0$ and $\overline{P}_{\rm diss} \geqslant 0$, as expected.

We will analyze the adiabatic dynamics of the charge and energy at the quantum dot and also the adiabatic regime of the charge and energy currents flowing in the normal leads. The latter can be carried out by using the nonequilibrium Green's function approach, as explained below.

D. Green's function approach

We present the general expressions to calculate the relevant time-dependent mean values of the observables defined in the previous sections by using the nonequilibrium Keldysh-Floquet Green's function formalism following Refs. [48,49] but now generalizing to the Nambu basis.

One of the observables we are interested in is the occupation of the quantum dot. In order to evaluate it, the starting point is the definition of the occupation matrix, with elements

$$n^{ij}_{d\sigma}(t) = -i[G^<_{d,\sigma}(t,t)]_{ij}, \quad (20)$$

which is defined from those of the lesser Nambu-Keldysh Green's function matrix

$$\hat G^<_{d,\sigma}(t,t') = i\begin{pmatrix}\langle d^\dagger_\sigma(t')d_\sigma(t)\rangle & \langle d_{\overline\sigma}(t')d_\sigma(t)\rangle\\ \langle d^\dagger_\sigma(t')d^\dagger_{\overline\sigma}(t)\rangle & \langle d_{\overline\sigma}(t')d^\dagger_{\overline\sigma}(t)\rangle\end{pmatrix}. \quad (21)$$

Here, $\overline\sigma$ denotes spin orientation opposite to σ. Particularly important for our purposes are the matrix elements

$$n_{d\sigma}(t) = n^{11}_{d\sigma}, \quad \eta_{d\sigma}(t) = n^{12}_{d\sigma}, \quad (22)$$

which define, respectively, the population of the dot with electrons with spin σ and with pairs induced at the quantum dot by proximity to the superconducting lead.

The lesser Green's function matrix $\hat G^<_{d,\sigma}(t,t')$ satisfies the Dyson equation

$$\hat G^<_{d,\sigma}(t,t') = \int dt_1dt_2\hat G^r_{d,\sigma}(t,t_1)\hat\Sigma^<(t_1-t_2)\hat G^a_{d,\sigma}(t_2,t'), \quad (23)$$

where $\hat G^r_{d,\sigma}(t,t_1) = [\hat G^a_{d,\sigma}(t_1,t)]^\dagger$ are the retarded and advanced Green's functions of the dot, while $\hat\Sigma^<(t_1,t_2)$ encodes the coupling self-energy for the dot reservoir. The Fourier transform for the coupling self-energy reads $\hat\Sigma^<(\varepsilon) = if(\varepsilon)\hat\Gamma(\varepsilon)$ and $\hat\Gamma(\varepsilon) = -2{\rm Im}[\hat\Sigma_S(\varepsilon)+\hat\Sigma_N(\varepsilon)]$, which are the coupling self-energies for the normal and superconducting contacts, and $f(\varepsilon) = 1/[1+\exp\beta\varepsilon]$ is the Fermi-Dirac function, where $\beta = 1/k_BT$, with T being the temperature and k_B being the Boltzmann constant (we recall that we have assumed $\mu_N = \mu_S = 0$).

Another observable we need is the charge current at the normal lead, which can be expressed in terms of Green's functions as follows:

$$I_N(t) = -\frac{2e}{\hbar}\sum_\sigma\int dt_1\int\frac{d\varepsilon}{2\pi}e^{-i\varepsilon(t_1-t)/\hbar} \times {\rm Re}\big[\hat G_{d,\sigma}(t,t_1)\hat\Sigma^<_N(\varepsilon)+\hat G^<_{d,\sigma}(t,t_1)\hat\Sigma^a_N(\varepsilon)\big]_{11}. \quad (24)$$

Similarly, the two terms in Eq. (14) defining the heat flux into the N reservoir $\dot Q_N(t)$ can also be expressed in terms of Green's functions,

$$J^E_N = -\frac{2}{\hbar}\sum_\sigma\int dt_1\int\frac{d\varepsilon}{2\pi}e^{-i\varepsilon(t_1-t)/\hbar}\,\varepsilon \times {\rm Re}\big[\hat G_{d,\sigma}(t,t_1)\hat\Sigma^<_N(\varepsilon)+\hat G^<_{d,\sigma}(t,t_1)\hat\Sigma^a_N(\varepsilon)\big]_{11}, \quad (25)$$

$$J^E_{cN} = \frac{2}{\hbar}\int\frac{d\varepsilon}{2\pi}f(\varepsilon)\,{\rm Re}\big[\partial_t\hat G_{d,\sigma}(t,\varepsilon)\hat\Gamma_N(\varepsilon)\big]_{11}. \quad (26)$$

Since the retarded and advanced dot Green's functions depend on two times, it is convenient to work in the mixed representation

$$\hat G^r_{d,\sigma}(t,t_1) = \int\frac{d\varepsilon}{2\pi}\hat G^r_{d,\sigma}(t,\varepsilon)e^{-i\varepsilon(t-t_1)/\hbar}, \quad (27)$$

where in terms of Fourier components it reads

$$\hat G^r_{d,\sigma}(t,t_1) = \sum_n e^{-in\Omega t}\int\frac{d\varepsilon}{2\pi}\hat G^r_{d,\sigma}(n,\varepsilon)e^{-i\varepsilon(t-t_1)/\hbar}. \quad (28)$$

Similarly, the ac electrical field reads as follows in the Fourier representation: $\hat V(t) = \sum_{n\neq0}[\hat V^+_n e^{-in\Omega t} + \hat V^-_n e^{in\Omega t}]$. Here, $\hat V^\pm_n$ are matrices in Nambu space with nonvanishing matrix elements,

$$[\hat V^+_n]_{11} = \frac{e}{\tau}\int_0^\tau dt\, e^{in\Omega t}V_g(t),$$
$$[\hat V^-_n]_{22} = -\frac{e}{\tau}\int_0^\tau dt\, e^{-in\Omega t}V_g(-t). \quad (29)$$

Finally, the Fourier transform in $t-t_1$ of the Green's function obeys the Dyson equation

$$\hat G^r_{d,\sigma}(t,\varepsilon) = \hat G_0(\varepsilon) + \sum_{s=\pm}\sum_n e^{-isn\Omega t} \times \hat G^r_{d,\sigma}(t,\varepsilon+sn\hbar\Omega)\hat V^s_n\hat G_0(\varepsilon). \quad (30)$$

1. Adiabatic expansion of the Green's function

For the adiabatic dynamics we just need a solution accurate up to $O(\Omega)$ for Eq. (30). Expanding the right-hand side of this equation in powers of Ω leads to

$$\hat G^r_{d,\sigma}(t,\varepsilon)[\hat G_0(\varepsilon)^{-1} - \hat V(t)] = \hat 1 + i\hbar\partial_\varepsilon\hat G^r_{d,\sigma}(t,\varepsilon)\frac{d\hat V(t)}{dt}. \quad (31)$$

The explicit solution to this equation reads

$$\hat G^r_{d,\sigma}(t,\varepsilon) \sim \hat G^r_{f,\sigma}(t,\varepsilon) + ie\hbar\partial_\varepsilon\hat G^r_{f,\sigma}(t,\varepsilon)\hat G^r_{f,\sigma}(t,\varepsilon)\dot V_g(t), \quad (32)$$

where $\hat G^r_{f,\sigma}(t,\varepsilon) = [\hat G_0(\varepsilon)^{-1} - \hat V(t)]^{-1}$ is the frozen dot Green's function.

2. *The frozen dot Green's function*

The frozen Green's function corresponds to the equilibrium problem defined by the Hamiltonian frozen at time t. It can be directly calculated by the equilibrium Dyson equation

$$\hat{G}^r_{f,\sigma}(t,\varepsilon)[\varepsilon\hat{1} - \hat{V}(t) - \hat{\Sigma}_N - \hat{\Sigma}_S] = \hat{1}. \tag{33}$$

We recall that $\hat{\Sigma}_N$ is the self-energy describing the coupling between the quantum dot and the normal reservoir and the matrix $\hat{\Sigma}_S$ describes the coupling to the superconducting one. In analogy to Eqs. (22), we define the frozen occupation matrix, with elements $[\hat{n}_{f,\sigma}(t)]_{ij} = -i[\hat{G}^<_{f,\sigma}(t,t)]_{ij}$, where the lesser Green's function matrix satisfies

$$\hat{G}^<_{f,\sigma}(t,\varepsilon) = \hat{G}^r_{f,\sigma}(t,\varepsilon)\hat{\Sigma}^<(\varepsilon)\big[\hat{G}^r_{f,\sigma}(t,\varepsilon)\big]^*. \tag{34}$$

In our calculations, we will use the following matrix elements, which define the frozen occupation of the quantum dot by particles and by induced pairs:

$$n^f_{d\sigma} = \hat{n}^{11}_{f\sigma}(t), \quad \eta^f_{d\sigma}(t) = \hat{n}^{12}_{f\sigma}(t). \tag{35}$$

The simplest model for the reservoirs corresponds to a constant density of states for the single-particle energies. This results in the following self-energy for the normal lead:

$$\hat{\Sigma}_N = \begin{pmatrix} -i\Gamma_N/2 & 0 \\ 0 & -i\Gamma_N/2 \end{pmatrix}. \tag{36}$$

Similarly, the self-energy for the superconducting lead reads

$$\hat{\Sigma}_S = -\frac{\Gamma_S\{\varepsilon\ \theta(\Delta - |\varepsilon|) + i|\varepsilon|\theta(|\varepsilon| - \Delta)\}}{2\sqrt{|\Delta^2 - (\varepsilon + i0^+)^2|}} \begin{pmatrix} 1 & \Delta/\varepsilon \\ \Delta/\varepsilon & 1 \end{pmatrix}. \tag{37}$$

Within this model for the self-energy, it is easy to show that the Green's function satisfies the properties presented in Appendix A.

In order to get explicit expressions we follow Ref. [50]. We name $[\hat{G}^r_{f,\sigma}(t,\varepsilon)]_{11} = -[\hat{G}^r_{f,\sigma}(t,-\varepsilon)]^*_{22} = G(t,\varepsilon)$ and $[\hat{G}^r_{f,\sigma}(t,\varepsilon)]_{12} = [\hat{G}^r_{f,\sigma}(t,\varepsilon)]^*_{21} = F(t,\varepsilon)$. In this case we get

$$G(t,\varepsilon) = \frac{1}{\varepsilon - eV_g(t) - \Sigma_{\rm eff}(t,\varepsilon)}, \tag{38}$$

where we have defined an effective self-energy $\Sigma_{\rm eff}(t,\varepsilon) = \Sigma^G(\varepsilon) + \Sigma^F(\varepsilon)^2\overline{g}(t,\varepsilon)$ with the help of

$$\Sigma^G(\varepsilon) = \sum_{\alpha=N,S}[\hat{\Sigma}_\alpha(\varepsilon)]_{11}, \quad \Sigma^F(\varepsilon) = \sum_{\alpha=N,S}[\hat{\Sigma}_\alpha(\varepsilon)]_{12}, \tag{39}$$

and $\overline{g}(t,\varepsilon) = 1/[\varepsilon + eV_g(-t) + \Sigma^G(-\varepsilon)^*]$. Finally, the anomalous propagator reads

$$F(t,\varepsilon) = -G(t,\varepsilon)\Sigma^F(\varepsilon)\overline{g}(t,\varepsilon). \tag{40}$$

IV. INSTANTANEOUS JOULE LAW FOR THE DOT DYNAMICS

Introducing the adiabatic expansion of the Green's function of Eq. (32) in the definition of the occupation of Eq. (20), we can identify the two contributions to the adiabatic dynamics of the occupation of the quantum dot. The frozen contribution is determined from the frozen Green's function. Conveniently, we define

$$\hat{\rho}_{f,\sigma}(t,\varepsilon) = i[\hat{G}_{f,\sigma}(t,\varepsilon) - \hat{G}_{f,\sigma}(t,\varepsilon)^*], \tag{41}$$

in terms of which the frozen occupation matrix reads

$$n^{ij}_{f\sigma}(t) = \int \frac{d\varepsilon}{2\pi} f(\varepsilon)[\hat{\rho}_{f,\sigma}(t,\varepsilon)]_{ij}. \tag{42}$$

The coefficient of the linear contribution in $\dot{V}_g$ of Eq. (16) becomes

$$\begin{aligned}\Lambda_\sigma(t) &= -2\hbar{\rm Im}\left[\int \frac{d\varepsilon}{2\pi} f(\varepsilon)\partial_\varepsilon\hat{G}_{f,\sigma}(t,\varepsilon)\hat{\rho}_{f,\sigma}(t,\varepsilon)\right]_{11} \\ &= -\frac{\hbar}{2}\int\frac{d\varepsilon}{2\pi}\partial_\varepsilon f(\varepsilon)\big\{[\hat{\rho}_{f,\sigma}(t,\varepsilon)]^2_{11} + [\hat{\rho}_{f,\sigma}(t,\varepsilon)]^2_{12}\big\}.\end{aligned} \tag{43}$$

Notice that in the last step we have integrated by parts and used $[\hat{G}_f(t,\varepsilon)]_{12} = [\hat{G}_f(t,\varepsilon)]_{21}$, which implies $[\hat{\rho}_{f,\sigma}(t,\varepsilon)]_{12} = [\hat{\rho}_{f,\sigma}(t,\varepsilon)]_{21}$. Hence, this coefficient can be split into two components as $\Lambda_\sigma(t) = \Lambda_{11,\sigma}(t) + \Lambda_{12,\sigma}(t)$, which at zero temperature are

$$\Lambda_{ij,\sigma}(t) = \frac{\hbar}{4\pi}[\hat{\rho}_{f,\sigma}(t,0)]^2_{ij}. \tag{44}$$

Now we evaluate the dissipative power from Eq. (18) by using Eq. (44). We see that this quantity also has two components, associated with those of $\Lambda_\sigma(t)$. We will show below that the component related to $\Lambda_{11,\sigma}(t)$ follows a normal instantaneous Joule law, and we label it $P^N_{\rm Joule}(t)$, while the one related to $\Lambda_{12,\sigma}(t)$ is denoted $\tilde{P}_{\rm Joule}(t)$ and follows an *anomalous Joule law*,

$$P_{\rm diss}(t) = P^N_{\rm Joule}(t) + \tilde{P}_{\rm Joule}(t), \tag{45}$$

with

$$\begin{aligned}P^N_{\rm Joule}(t) &= \frac{e^2\hbar}{4\pi}\sum_\sigma[\hat{\rho}_{f,\sigma}(t,0)]^2_{11}\dot{V}^2_g(t), \\ \tilde{P}_{\rm Joule}(t) &= \frac{e^2\hbar}{4\pi}\sum_\sigma[\hat{\rho}_{f,\sigma}(t,0)]^2_{12}\dot{V}^2_g(t)\,.\end{aligned} \tag{46}$$

In order to make the Joule law explicit, we proceed to relate the two components of the dissipative power equation (45) to the dot charge dynamics. To this end, we analyze the time evolution of the dot charge up to $O(\dot{V}_g(t))$. This leads to the purely ac charge current, which reads

$$\frac{dq_{d\sigma}(t)}{dt} = e\dot{n}^f_{d\sigma}(t) = C_\sigma(t)\dot{V}_g(t). \tag{47}$$

Here, we can identify the nonlinear capacitance of each spin channel $C_\sigma(t) = e\partial n^f_{d\sigma}(t)/\partial V_g$. In addition, the dynamics of the charge and heat involves the dynamics of the induced pairs at the quantum dot by proximity to the superconductor. The latter is $\eta^f_{d\uparrow}(t) = \langle d^\dagger_\uparrow d^\dagger_\downarrow\rangle = \langle d_\downarrow d_\uparrow\rangle = -\eta^f_{d\downarrow}(t)$. The corresponding charge fluctuation reads

$$\frac{dq^\eta_{d\sigma}(t)}{dt} = e\dot{\eta}^f_{d\sigma}(t) = \pm\partial\eta^f_{d\uparrow}(t)/\partial\dot{V}_g(t), \tag{48}$$

where the upper and lower signs correspond to $\sigma = \uparrow,\downarrow$, respectively. Importantly, we get two contributions with opposite

signs in (48), which reflects the fact that a pair fluctuation implies a simultaneous flux of electrons and holes. As a consequence, the net induced current between the dot and reservoirs vanishes, although the process leads to energy dissipation in the form of a Joule law for the electrons and for the holes. Notice that each of the contributions $\partial\eta^{f}_{d\sigma}(t)/\partial V_g$ can be positive or negative, depending on the occupation of the quantum dot. However, as they have opposite signs, the net contribution cancels when they are added. For this reason, we find it convenient to define the "anomalous capacitance" as $\tilde{C}(t) = e|\partial\eta^{f}_{d\uparrow}(t)/\partial V_g|$ and redefine the induced-pair charge fluctuations as

$$\frac{d\tilde{q}_{d\sigma}(t)}{dt} = \pm\tilde{C}(t)\dot{V}_g(t), \tag{49}$$

which satisfies $\sum_\sigma d\tilde{q}_{d\sigma}(t)/dt = \sum_\sigma dq^{\eta}_{d\sigma}(t)/dt = 0$.

In order to compute the capacitances we evaluate the dynamics of the dot charge at first order in $\dot{V}_g(t)$. Then, starting from

$$\begin{aligned}\dot{n}^{ij}_{d\sigma}(t) &= \int \frac{d\varepsilon}{2\pi} f(\varepsilon)\frac{d[\hat{\rho}_{f,\sigma}(t,\varepsilon)]_{ij}}{dt}\\ &= e\int \frac{d\varepsilon}{2\pi}\partial_\varepsilon f[\hat{\rho}_{f,\sigma}(t,\varepsilon)]_{ij}\dot{V}_g\end{aligned} \tag{50}$$

and comparing Eq. (50) with Eqs. (47) and (49), in the zero-temperature limit we find

$$C_\sigma(t) = \frac{e^2}{2\pi}[\hat{\rho}_{f,\sigma}(t,0)]_{11}, \quad \tilde{C}(t) = \frac{e^2}{2\pi}|[\hat{\rho}_{f,\uparrow}(t,0)]_{12}|. \tag{51}$$

The dot charge dynamics [see Eq. (47)] and the time evolution for the pair-density charge [see Eq. (49)] together with Eq. (51) can now be related to the normal and anomalous Joule components of the dissipative power [see Eq. (45)] according to

$$\begin{aligned}P^{N}_{\rm Joule}(t) &= R_0\sum_\sigma\left[\frac{dq_{d\sigma}(t)}{dt}\right]^2,\\ \tilde{P}_{\rm Joule}(t) &= R_0\sum_\sigma\left[\frac{d\tilde{q}_{d\sigma}(t)}{dt}\right]^2,\end{aligned} \tag{52}$$

with a constant and universal quantum resistance $R_0 = h/2e^2$. While in the first term of Eq. (52) the label σ represents fluxes of charges with different spin components, in the second term it actually represents the two opposite charges for the electrons and holes. We notice that the above dynamics can be described by the circuit sketched in Fig. 1(b), which corresponds to a generalization of the RC circuit of a driven quantum dot connected to a normal reservoir. There are four different channels that run in parallel; each channel has its own capacitance. We will see that the normal capacitance $C_\sigma(t)$ has contributions associated with normal transport as well as Andreev processes, while the anomalous capacitance accounts for the induced Cooper pair fluctuation. The latter process involves opposite currents of electrons and holes, which do not produce any net current. Each of these channels dissipates energy in the form a Joule law with the universal Büttiker resistance R_0. This result holds for arbitrary amplitude of the driving potential provided that the driving frequency is low enough and the reservoirs have $T = 0$.

V. INSTANTANEOUS JOULE LAW AT THE NORMAL CONTACT

We recall that we are considering the chemical potential within the superconducting gap. This regime is interesting because the heat flux to the superconducting reservoir vanishes, which means that the dissipated energy flows only into the normal lead. In this situation we can get analytic expressions for the currents into the normal lead in the adiabatic regime. Our aim now is to verify that such heat flux also obeys an instantaneous Joule law with Büttiker universal resistance R_0. We follow Refs. [48,49] to derive the charge and heat flow at the normal contact in the adiabatic approximation. Details are presented in Appendix B. We arrive at the expression for the heat current up to second order in $\dot{V}_g(t)$ [equivalent to up to $O(\Omega^2)$]. Such a flux comprises two different contributions,

$$\dot{Q}_N(t) = \Lambda^{(1)}_N(t)(t)\dot{V}_g(t) + \Lambda^{(2)}_N(t)\dot{V}_g(t)^2 + O[V_g(t)^3] + \cdots. \tag{53}$$

$\Lambda^{(1)}_N(t)$ is first order in the ac frequency Ω and vanishes at zero temperature. The other term is the second-order contribution and reads, for the zero-temperature limit,

$$\dot{Q}_N(t) \simeq \frac{e^2\hbar}{4\pi}\sum_\sigma\left\{[\rho_{f,\sigma}(t,0)]^2_{11} + [\rho_{f,\sigma}(t,0)]^2_{12}\right\}\dot{V}_g(t)^2. \tag{54}$$

Notice that Eq. (54) is precisely the dissipated power $P_{\rm Joule}(t)$ given by Eq. (45). This result implies that the dissipative power coincides with the heat flow expression in the normal contact. In addition, it is important to emphasize that such heat current at the normal lead has been computed considering the contribution of the energy reactance; see the second term of Eq. (14).

Finally, we calculate the expression for the charge current at the normal electrode at zero temperature, which is calculated from Eq. (7), and it reads

$$I_N(t) = \frac{e^2}{2\pi}\sum_\sigma\{[\rho_{f,\sigma}(t,0)]_{11} + [\rho_{f,\sigma}(t,0)]_{12}\}\dot{V}_g(t). \tag{55}$$

This again confirms the instantaneous Joule law [see Eqs. (54) and (55)].

Therefore, the analysis of the fluxes in the normal lead confirms the description of the dissipation in our setup in terms of a circuit composed of two parallel subcircuits; each of them corresponds to a RC circuit composed of the usual capacitance C and R_0 and the anomalous capacitance $\tilde{C}$ and again R_0. The circuit picture reflects the fact that the normal reservoir effectively receives the charge flowing through all the resistive elements depicted in Fig. 1(b) that comes from (i) the normal transmission, (ii) the Andreev processes, and, finally, (iii) the Cooper pair fluctuation. All these transport events are the result of quasiparticle excitations that lead to energy dissipation. In the next section we will analyze these contributions in more detail.

VI. ANALYSIS OF THE CAPACITANCES AND THE DISSIPATED POWER

We now show results illustrating the behavior of the capacitances, which determine the behavior of the charge and heat currents between the quantum dot and the reservoir. Substituting the dot Green function [see Eq. (38)] in the expression for the dot density of states [see Eq. (41)], we explicitly see that the capacitance for each spin channel given by Eq. (51) has two different contributions at zero temperature:

$$C_\sigma(t) \equiv C(t) = C_{\rm N}(t) + C_{\rm And}(t). \tag{56}$$

We identify them as normal ($C_{\rm N}$) and Andreev-type ($C_{\rm And}$) processes. They can be expressed in terms of the Green's functions and self-energies previously defined [see Eq. (38)] as follows:

$$\begin{aligned} C_{\rm N}(t) &= \frac{e^2}{2\pi}\Gamma^G(0)|G(t,0)|^2, \\ C_{\rm And}(t) &= \frac{e^2}{2\pi}\Gamma^G(0)|G(t,0)\Sigma^F(0)\overline{g}(t,0)|^2, \end{aligned} \tag{57}$$

with $\Gamma^G(0) = -2{\rm Im}[\Sigma^G(0)]$. Notice that the normal contribution is directly related to the normal part of the spectral function and exactly reduces to the capacitance of the quantum dot connected to a single normal lead in the limit of vanishing coupling to the superconducting one. Instead, the contribution $C_{\rm And}(t)$ is proportional to the coupling to the superconducting lead and involves high-order scattering processes, characteristic of the Andreev reflection. The anomalous capacitance is

$$\tilde{C}(t) = \frac{e^2}{\pi}|{\rm Im}[F(t,0)]|. \tag{58}$$

The latter is proportional to the absolute value of the spectral function of the anomalous Green's function [see Eq. (40)], which is positive (negative) for $V_g(t) > 0$ [$V_g(t) < 0$].

The behavior of the different capacitances is illustrated in Fig. 2. Two different cases are shown, namely, the superconducting-dominant case when $\Gamma_S > \Gamma_N$ (left panels in Fig. 2 with $\Gamma_N = \Gamma_S/4$) and the case when both tunnel couplings are equal $\Gamma_N = \Gamma_S$ (right panels in Fig. 2). In the simplest situation where the quantum dot is coupled only to the normal electrode and without driving, there is a single level at the Fermi energy $\mu_N = 0$. The additional coupling to the superconducting electrode induces local pairing correlations in the quantum dot. Then, the original single-dot level splits into two Andreev quasiparticle states in which the magnitude of the splitting depends on the relative value of Γ_S/Γ_N. Since the behavior of the capacitance is determined by the spectral properties of the quantum dot, these features are clearly identified in Fig. 2. In fact, for the superconducting-dominant case the dot spectral density exhibits a larger level splitting in comparison to the case where both lead-dot couplings are similar. As a function of time, the gate voltage moves upwards and downwards. The Andreev quasiparticle energy levels and the capacitances have weights when the dot spectral functions have weight at the Fermi energy $\mu = 0$. In addition, we observe that the normal capacitance $C_{\rm N}(t)$ follows the profile of the Andreev levels, while the capacitance associated with Andreev reflection processes shows an additional weight between the

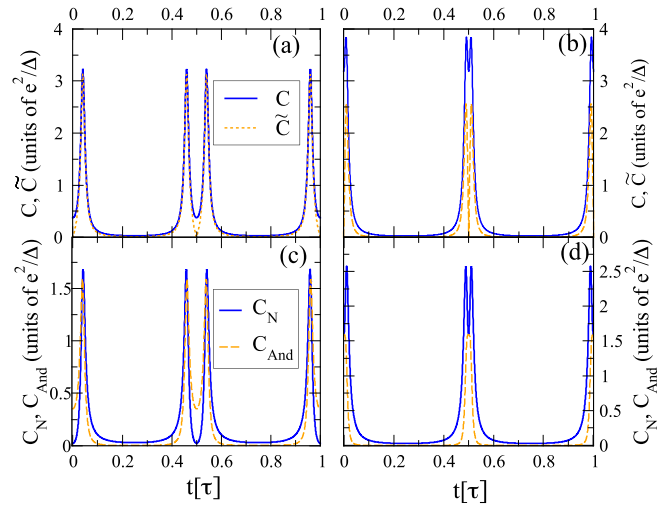

FIG. 2. Capacitances of the driven quantum dot for $\Gamma_N = \Gamma_S/4 = \Delta/10$ (left panels) and $\Gamma_N = \Gamma_S = \Delta/10$ (right panels). Times are expressed in units of the driving period. The amplitude of the driving gate voltage is $V_0 = 0.8\Delta$. (a) and (b) Solid lines and dashed lines correspond to $C(t)$ and $\tilde{C}(t)$. (c) and (d) Solid lines and dashed lines correspond to $C_{\rm N}(t)$ and $C_{\rm And}(t)$.

two Andreev peaks. We observe that the anomalous capacitance follows the spectral features of the anomalous Green's function with resonances at the Andreev quasiparticle states. In addition, the anomalous Green's function changes sign every time that $V_g(t) = 0$; hence, $\tilde{C}(t) = 0$ at those times.

Every time $C(t)$ and $\dot{V}_g(t)$ are finite, a charge current establishes between the quantum dot and the normal lead. This current has normal and Andreev components for each spin component, leading to a net flux

$$\sum_\sigma \frac{dq_\sigma(t)}{dt} = 2[C_{\rm N}(t) + C_{\rm And}(t)]\dot{V}_g(t). \tag{59}$$

This flux leads to dissipation of energy following the Joule law

$$P^N_{\rm Joule}(t) = 2R_0[C_{\rm N}(t) + C_{\rm And}(t)]^2\dot{V}_g(t)^2. \tag{60}$$

The contribution due to the fluctuation of the induced pairing leads to opposite particle and hole fluxes described by Eq. (49) and has an associated net vanishing current,

$$\sum_\sigma \frac{d\tilde{q}_{d\sigma}(t)}{dt} = 0. \tag{61}$$

This process contributes, however, to the dissipation of energy in the form of an anomalous Joule law,

$$\tilde{P}_{\rm Joule}(t) = 2R_0\tilde{C}(t)^2\dot{V}_g(t)^2. \tag{62}$$

The different contributions to the dissipated power are shown in Fig. 3. Both contributions are peaked at the times where the energy levels of the Andreev states get aligned with the chemical potential of the leads. Due to the contribution of the Andreev capacitance, there is a finite current and Joule dissipation in the time intervals between these peaks in $P_{\rm Joule}(t)$. The anomalous dissipation $\tilde{P}_{\rm Joule}(t)$ due to the disruption or formation of induced pairs vanishes exactly at the center of the gap between the pair of Andreev peaks.

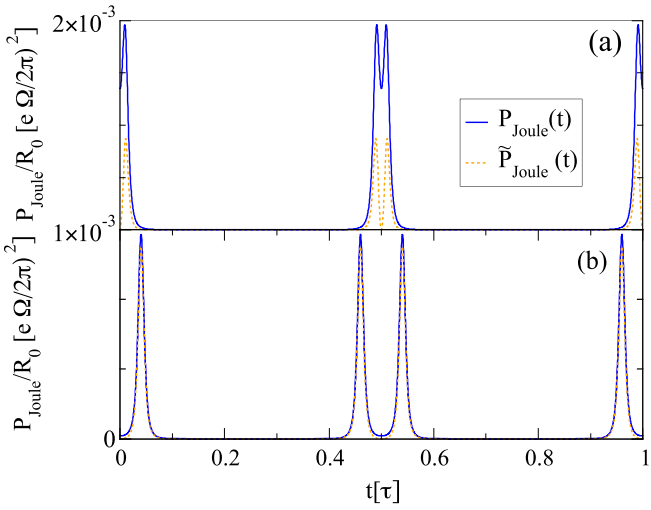

FIG. 3. Dissipated power of the driven quantum dot for $\Gamma_N = \Gamma_S = \Delta/10$ (top) and $\Gamma_N = \Gamma_S/4 = \Delta/10$ (bottom). Solid lines and dashed lines correspond to the contribution of the ordinary, $P^N_{\rm Joule}(t)$, and anomalous, $\tilde{P}_{\rm Joule}(t)$, components of the Joule law, respectively. Other details are the same as for Fig. 2.

VII. CONCLUSIONS

We have investigated the charge and energy dynamics of a driven quantum dot in contact with superconducting and normal leads. We have focused on the adiabatic regime, relevant for low-frequency driving, with reservoirs at $T = 0$. We have derived the dissipative power from (i) the dot charge dynamics and, equivalently, (ii) the heat flow at the N contact that accounts for the reactance contribution from the tunneling barriers. In addition, the charge current is calculated from (i) the time derivative of the dot charge and (ii) the charge current flow exiting the normal contact. For both cases a dynamical Joule law is established, leading to a universal nonlinear charge resistance $R_0 = h/2e^2$. In this scenario we have shown that the Joule dynamics law may be described in terms of the RC circuit of Fig. 1(b). According to Fig. 1(b) the capacitance C takes into account the normal and Andreev processes, whereas $\tilde{C}$ accounts for the generation of pairs. Remarkably, the current due to the pair generation vanishes as a result of the cancellation of electron and hole flows. However, it is important to highlight that such pair fluctuation processes contribute to the heat dissipation through an instantaneous Joule heating. The universality of the Joule law ruled by the Büttiker resistance R_0 is expected to be valid for low enough temperatures and does not rely on specific parameters of the system. In particular, it is expected to be valid for interacting quantum dots in the Fermi liquid regime as in Refs. [14,15,31]. At finite temperatures, however, corrections to R_0 are expected, as discussed in Ref. [33].

ACKNOWLEDGMENTS

L.A. thanks A. Levy Yeyati for reading the manuscript and interesting comments. L.A. acknowledges the support of the Alexander von Humboldt Foundation, as well as CONICET, UBACyT, and MinCyT from Argentina. R.L. acknowlegdes the support offered by MINECO Grants No. FIS2014-52564 and No. MAT2017-82639.

APPENDIX A: PROPERTIES AND IDENTITIES OF THE FROZEN GREEN'S FUNCTION

The frozen Green's function satisfies the following properties:

$$\hat{\rho}_{f,\sigma}(t,\varepsilon) = i[\hat{G}_{f,\sigma}(t,\varepsilon) - \hat{G}_{f,\sigma}(t,\varepsilon)^*] = \hat{G}_{f,\sigma}(t,\varepsilon)\hat{\Gamma}(\varepsilon)\hat{G}_{f,\sigma}(t,\varepsilon)^\dagger, \tag{A1}$$

$$\partial_\varepsilon \hat{G}_{f,\sigma}(t,\varepsilon) \simeq -\hat{G}_{f,\sigma}(t,\varepsilon)^2, \quad \frac{d\hat{G}_{f,\sigma}(t,\varepsilon)}{dt} = \hat{G}_{f,\sigma}(t,\varepsilon)\hat{G}_{f,\sigma}(t,\varepsilon)e\dot{V}_g(t) \simeq -e\partial_\varepsilon \hat{G}_f(t,\varepsilon)\dot{V}_g(t), \tag{A2}$$

where $\hat{\Gamma}(\varepsilon) = i[\hat{\Sigma}^r(\varepsilon) - \hat{\Sigma}^r(\varepsilon)^*]$. In the last identities, we have assumed that we can neglect the dependence on ε of $\hat{\Sigma}$, which is a valid assumption for models of reservoirs introduced in Sec. III D 2.

APPENDIX B: ADIABATIC EXPANSION FOR THE CHARGE AND HEAT CURRENTS INTO THE N RESERVOIR FOR SUBGAP DRIVING

The charge and energy currents in the the normal lead are defined, respectively, in Eqs. (24) and (25). Substituting Eq. (28) in these expressions and using identities for the Green's functions along the same steps as presented in Refs. [32,33] but expressed in the Nambu representation, we get

$$I_N(t) = \frac{e}{\hbar}\sum_\sigma \sum_l e^{-il\Omega t}\int \frac{d\varepsilon}{2\pi}\Bigg(\hat{\Gamma}_{\rm N}(\varepsilon)\Big\{i\hat{G}^*_{d,\sigma}(-l,\varepsilon)[f(\varepsilon) - f(\varepsilon - l\hbar\Omega)]$$

$$+ \sum_n \sum_{\beta=N,S}[f(\varepsilon + n\hbar\Omega) - f(\varepsilon)]\hat{G}_{d\sigma}(l+n,\varepsilon)\hat{\Gamma}_\beta(\varepsilon)\hat{G}^*_{d,\sigma}(n,\varepsilon)\Big\}\Bigg)_{11},$$

$$\dot{Q}_N(t) = \frac{1}{\hbar}\sum_{\sigma}\sum_{l} e^{-il\Omega t}\int \frac{d\varepsilon}{2\pi}\left(\hat{\Gamma}_{\rm N}(\varepsilon)\left\{ i\hat{G}^{*}_{d,\sigma}(-l,\varepsilon)\left(\varepsilon - \frac{l\hbar\Omega}{2}\right)[f(\varepsilon) - f(\varepsilon - l\hbar\Omega)]\right.\right.$$

$$\left.\left. - \sum_{n}\sum_{\beta=N,S}\left[\varepsilon + \left(\frac{l}{2}+n\right)\hbar\Omega\right][f(\varepsilon+n\hbar\Omega) - f(\varepsilon)]\hat{G}_{d,\sigma}(l+n,\varepsilon)\hat{\Gamma}_{\beta}(\varepsilon)\hat{G}^{*}_{d,\sigma}(n,\varepsilon)\right\}\right)_{11}. \tag{B1}$$

In order to get the adiabatic expansion for the currents, we have to introduce Eq. (B1), the adiabatic expansion of the Green's function defined in Eq. (32), and the corresponding expansion for the Fermi-Dirac distribution function

$$f(\varepsilon - l\hbar\Omega) = f(\varepsilon) - l\hbar\Omega\frac{\partial f}{\partial\varepsilon} + \frac{1}{2}(l\hbar\Omega)^2\frac{\partial^2 f}{\partial\varepsilon^2}. \tag{B2}$$

Then, we keep the terms of the charge current up to $(\hbar\Omega)$ and of the heat current in the first and second orders in $\hbar\Omega$. Here, we also use the fact that within the gap, the density of states of the superconducting lead vanishes; hence, $\Gamma_S \sim 0$ for $|\varepsilon| < \Delta$. The results are the following:

$$I^{(1)}_N(t) = e^2\sum_{\sigma}\int\frac{d\varepsilon}{2\pi}\partial_\varepsilon f(\varepsilon)\{[\rho_{f,\sigma}(t,\varepsilon)]_{11} + [\rho_{f,\sigma}(t,\varepsilon)]_{12}\}\dot{V}_g(t),$$

$$\dot{Q}^{(1)}_N(t) \simeq -e\hbar\sum_{\sigma}\int\frac{d\varepsilon}{2\pi}\varepsilon\ \partial_\varepsilon f(\varepsilon)\{[\rho_{f,\sigma}(t,\varepsilon)]_{11} + [\rho_{f,\sigma}(t,\varepsilon)]_{12}\}\dot{V}_g(t),$$

$$\dot{Q}^{(2)}_N(t) \simeq -\frac{\hbar}{2}\sum_{\sigma,\beta}\int\frac{d\varepsilon}{2\pi}\partial_\varepsilon f(\varepsilon)[\partial_t\hat{G}_{f,\sigma}(t,\varepsilon)\hat{\Gamma}_{\beta}(\varepsilon)\partial_t\hat{G}^{*}_{f,\sigma}(t,\varepsilon)]_{11}$$

$$= -\frac{e^2\hbar}{2}\sum_{\sigma}\int\frac{d\varepsilon}{2\pi}\partial_\varepsilon f(\varepsilon)\{[\rho_{f,\sigma}(t,\varepsilon)]^2_{11} + [\rho_{f,\sigma}(t,\varepsilon)]^2_{12}\}\dot{V}_g(t)^2. \tag{B3}$$

In the last equation, we have dropped those contributions to $\dot{Q}^{(2)}_{\rm N}(t)$ that vanish at temperature $T = 0$. Notice that $\dot{Q}^{(1)}_{\rm N}(t)$ also vanishes at $T = 0$.

[1] G. Fève, A. Mahé, J.-M. Berroir, T. Kontos, B. Placais, C. Glattli, A. Cavanna, B. Etienne, and Y. Jin, An on-demand coherent single-electron source, Science **316**, 1169 (2007).

[2] M. Büttiker, A. Prêtre, and H. Thomas, Dynamic Conductance and the Scattering Matrix of Small Conductors, Phys. Rev. Lett. **70**, 4114 (1993).

[3] A. Prêtre, H. Thomas, and M. Büttiker, Dynamic admittance of mesoscopic conductors: Discrete-potential model, Phys. Rev. B **54**, 8130 (1996).

[4] M. Büttiker, H. Thomas, and A. Prêtre, Mesoscopic capacitors, Phys. Lett. A **180**, 364 (1993).

[5] J. Gabelli, G. Fève, J.-M. Berroir, B. Placais, A. Cavanna, B. Etienne, Y. Jin, and D. C. Glattli, Violation of Kirchhoff's laws for a coherent RC circuit, Science **313**, 499 (2006).

[6] J. Gabelli, G. Féve, J.-M. Berroir, and B. Placais, A coherent RC circuit, Rep. Prog. Phys. **75**, 126504 (2012).

[7] F. D. Parmentier, E. Bocquillon, J.-M. Berroir, D. C. Glattli, B. Plaçais, G. Fève, M. Albert, C. Flindt, and M. Büttiker, Current noise spectrum of a single-particle emitter: Theory and experiment, Phys. Rev. B **85**, 165438 (2012).

[8] B. J. van Wees, H. van Houten, C. W. J. Beenakker, J. G. Williamson, L. P. Kouwenhoven, D. van der Marel, and C. T. Foxon, Quantized Conductance of Point Contacts in a Two-Dimensional Electron Gas, Phys. Rev. Lett. **60**, 848 (1988).

[9] K. V. Klitzing, G. Dorda, and M. Pepper, New Method for High-Accuracy Determination of the Fine-Structure Constant Based on Quantized Hall Resistance, Phys. Rev. Lett. **45**, 494 (1980).

[10] S. E. Nigg, R. López, and M. Büttiker, Mesoscopic Charge Relaxation, Phys. Rev. Lett. **97**, 206804 (2006).

[11] Z. Ringel, Y. Imry, and O. Entin-Wohlman, Delayed currents and interaction effects in mesoscopic capacitors, Phys. Rev. B **78**, 165304 (2008).

[12] C. Mora and K. Le Hur, Universal resistances of the quantum resistance-capacitance circuit, Nat. Phys. **6**, 697 (2010).

[13] Y. Hamamoto, T. Jonckheere, T. Kato, and T. Martin, Dynamic response of a mesoscopic capacitor in the presence of strong electron interactions, Phys. Rev. B **81**, 153305 (2010).

[14] M. Lee, R. López, M.-S. Choi, T. Jonckheere, and T. Martin, Effect of many-body correlations on mesoscopic charge relaxation, Phys. Rev. B **83**, 201304 (2011).

[15] M. Filippone and C. Mora, Fermi liquid approach to the quantum RC circuit: Renormalization-group analysis of the Anderson and Coulomb blockade models, Phys. Rev. B **86**, 125311 (2012).

[16] G. Rosselló, R. López, and J. S. Lim, Time-dependent heat flow in interacting quantum conductors, Phys. Rev. B **92**, 115402 (2015).

[17] P. Dutt, T. L. Schmidt, C. Mora, and K. Le Hur, Strongly correlated dynamics in multichannel quantum RC circuits, Phys. Rev. B **87**, 155134 (2013).

[18] O. Kashuba, H. Schoeller, and J. Splettstoesser, Nonlinear adiabatic response of interacting quantum dots, Eur. Phys. Lett. **98**, 57003 (2012).

[19] M. Filippone, K. Le Hur, and C. Mora, Giant Charge Relaxation Resistance in the Anderson Model, Phys. Rev. Lett. **107**, 176601 (2011).
[20] M. Filippone, K. Le Hur, and C. Mora, Admittance of the SU(2) and SU(4) Anderson quantum *RC* circuits, Phys. Rev. B **88**, 045302 (2013).
[21] H. Shiba, The korringa relation for the impurity nuclear spin-lattice relaxation in dilute kondo alloys, Prog. Theor. Phys. **54**, 967 (1975).
[22] M. Moskalets, P. Samuelsson, and M. Büttiker, Quantized Dynamics of a Coherent Capacitor, Phys. Rev. Lett. **100**, 086601 (2008).
[23] S. Ol'khovskaya, J. Splettstoesser, M. Moskalets, and M. Büttiker, Shot Noise of a Mesoscopic Two-Particle Collider, Phys. Rev. Lett. **101**, 166802 (2008).
[24] J. Splettstoesser, S. Ol'khovskaya, M. Moskalets, and M. Büttiker, Electron counting with a two-particle emitter, Phys. Rev. B **78**, 205110 (2008).
[25] G. Haack, M. Moskalets, and M. Büttiker, Glauber coherence of single electron sources, Phys. Rev. B **87**, 201302(R) (2013).
[26] M. Moskalets, G. Haack, and M. Büttiker, Single-electron source: Adiabatic versus non-adiabatic emission, Phys. Rev. B **87**, 125429 (2013).
[27] J. Keeling, A. V. Shytov, and L. S. Levitov, Coherent Particle Transfer in an On-Demand Single-Electron Source, Phys. Rev. Lett. **101**, 196404 (2008).
[28] D. Litinski, P. W. Brouwer, and M. Filippone, The interacting mesoscopic capacitor out of equilibrium, Phys. Rev. B **96**, 085429 (2017).
[29] I. Aleiner, P. Brouwer, and L. Glazman, Quantum effects in Coulomb blockade, Phys. Rep. **358**, 309 (2002).
[30] M. I. Alomar, J. S. Lim, and D. Sánchez, Coulomb-blockade effect in nonlinear mesoscopic capacitors, Phys. Rev. B **94**, 165425 (2016).
[31] J. Romero, P. Roura-Bas, A. Aligia, and L. Arrachea, Nonlinear charge and energy dynamics of an adiabatic driven interacting quantum dot, Phys. Rev. B **95**, 235117 (2017).
[32] M. F. Ludovico, J. S. Lim, M. Moskalets, L. Arrachea, and D. Sánchez, Dynamical energy transfer in ac-driven quantum systems, Phys. Rev. B **89**, 161306(R) (2014).
[33] M. F. Ludovico, M. Moskalets, D. Sánchez, and L. Arrachea, Dynamics of energy transport and entropy production in ac-driven quantum electron systems, Phys. Rev. B **94**, 035436 (2016).
[34] M. F. Ludovico, L. Arrachea, M. Moskalets, and D. Sánchez, Periodic energy transport and entropy production in quantum electronics, Entropy **18**, 419 (2016).
[35] M. F. Ludovico, L. Arrachea, M. Moskalets, and D. Sánchez, Probing the energy reactance with adiabatically driven quantum dots, Phys. Rev. B **97**, 041416(R) (2018).
[36] M. R. Gräber, T. Nussbaumer, W. Belzig, and C. Schönenberger, Quantum dot coupled to a normal and a superconducting lead, Nanotechnology **15**, S479 (2004).
[37] R. S. Deacon, Y. Tanaka, A. Oiwa, R. Sakano, K. Yoshida, K. Shibata, K. Hirakawa, and S. Tarucha, Kondo-enhanced Andreev transport in single self-assembled InAs quantum dots contacted with normal and superconducting leads, Phys. Rev. B **81**, 121308(R) (2010).
[38] S. De Franceschi, L. Kouwenhoven, C. Schonenberger, and W. Wernsdorfer, Hybrid superconductor-quantum dot devices, Nat. Nanotechnol. **5**, 703 (2010).
[39] A. Martín-Rodero and A. Levy Yeyati, Josephson and Andreev transport through quantum dots, Adv. Phys. **60**, 899 (2011).
[40] L. Li, Z. Cao, T.-F. Fang, H.-G. Luo, and W.-Q. Chen, Kondo screening of Andreev bound states in a normal metal–quantum dot–superconductor system, Phys. Rev. B **94**, 165144 (2016).
[41] M. Blaauboer, Charge pumping in mesoscopic systems coupled to a superconducting lead, Phys. Rev. B **65**, 235318 (2002).
[42] M. Governale, F. Taddei, F. W. J. Hekking, and R. Fazio, Adiabatic Pumping in a Superconductor-Normal-Superconductor Weak Link, Phys. Rev. Lett. **95**, 256801 (2005).
[43] J. Splettstoesser, M. Governale, J. König, F. Taddei, and R. Fazio, Pumping through a quantum dot in the proximity of a superconductor, Phys. Rev. B **75**, 235302 (2007).
[44] L. E. Bruhat, J. J. Viennot, M. C. Dartiailh, M. M. Desjardins, T. Kontos, and A. Cottet, Cavity Photons as a Probe for Charge Relaxation Resistance and Photon Emission in a Quantum Dot Coupled to Normal and Superconducting Continua, Phys. Rev. X **6**, 021014 (2016).
[45] G. E. Blonder, M. Tinkham, and T. M. Klapwijk, Transition from metallic to tunneling regimes in superconducting microconstrictions: Excess current, charge imbalance, and supercurrent conversion, Phys. Rev. B **25**, 4515 (1982).
[46] F. Covito, F. G. Eich, R. Tuovinen, M. A. Sentef, A. Rubio, Transient charge and energy flow in the wide-band limit, J. Chem. Theory Comput. **14**, 2495 (2018).
[47] M. F. Ludovico, F. Battista, F. von Oppen, and L. Arrachea, Adiabatic response and quantum thermoelectrics for ac-driven quantum systems, Phys. Rev. B **93**, 075136 (2016).
[48] L. Arrachea, Exact Green's function renormalization approach to spectral properties of open quantum systems driven by harmonically time-dependent fields, Phys. Rev. B **75**, 035319 (2007).
[49] L. Arrachea and M. Moskalets, Relation between scattering-matrix and Keldysh formalisms for quantum transport driven by time-periodic fields, Phys. Rev. B **74**, 245322 (2006).
[50] L. Arrachea, Stationary transport in mesoscopic hybrid structures with contacts to superconducting and normal wires: A Green's function approach for multiterminal setups, Phys. Rev. B **79**, 104513 (2009).